RESEARCH REPORT

Viatcheslav S. Solomatov, Visiting Professor, July 2011 - November 2011

1. Gain size variations and seismic anomalies beneath oceanic lithosphere and subducting slabs

Introduction

The importance of grain size variations in the Earth's mantle was realized over two decades ago (e.g., Karato 1984). Grain size variations affect the dynamic processes, including the rate of secular cooling of the planet (Solomatov 2001), the structure of mantle plumes (Korenaga 2005), slab weakening (Riedel and Karato 1997), chemical mixing (Hall et al. 2003; Solomatov and Reese 2008), subduction initiation (Bercovici and Ricard 2008) and fluid transport (Wada et al. 2011). Grain size variations also affect the seismic attenuation and seismic velocities (Minster and Anderson 1981; Karato 1993, 2008; Faul and Jackson 2005; Jackson and Faul 2010). Here we report some preliminary results regarding grain size evolution and its effect on seismic velocities below the oceanic lithosphere. The lithosphere-asthenosphere boundary (LAB) region is especially interesting because there are important seismic constrains on this region (Kawakatsu et al 2009) and also, as we show below, the grain size variations are expected to be the largest there.

Stresses due to lithospheric thickness variation

Previous analyses of the rheology and grain size variations within the lithosphere and asthenosphere considered one-dimensional, constant shear stress channel flow models (Podolefsky et al 2004, Behn et al 2009). We use fully dynamic models (Solomatov and Moresi 2000; Honda 2009). One of the major differences from the previous models is that the viscous stresses in the lithosphere and the subducting slab vary by several orders of magnitude (Figs. 1 and 2).

Fig.1: Temperature field in the presence of sublithospheric small-scale convection. Note large variations in the lithosphere-asthenosphere boundary which is represented by a white region separating the cold (blue) lithosphere and hot (red) asthenosphere. These variations are the main source of stresses in the LAB region.
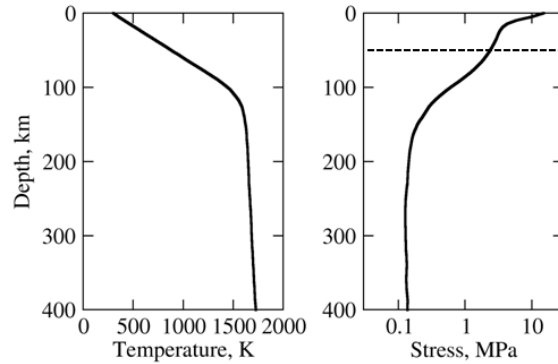

Fig.2: Horizontally averaged temperature and viscous stress profiles in the upper part of the convective mantle. The dashed line indicates an approximate limit of applicability of stress calculations because of more complex rheologies (especially brittle fracture and elasticity) than the simple viscous behavior assumed here.

Grain size variation

The grain size in the steady-state dynamic recrystallization regime varies inversely with stress (Karato 2008), and thus the stress variations produce correspondingly large variations in the grain size. Recent modifications of scaling laws for dynamic recrystallization (de Bresser et al 1998; Shimizu, 1998, 2008, 2011; Austin and Evans 2007) suggest that the grain size may depend not only on stress but also exponentially on temperature, although the magnitude and even the sign of this effect depends on the poorly constrained rheological parameters. With all the uncertainties, it nevertheless seems likely that steep grain size gradients form in the sublithospheric region, especially in the vicinity of the lithosphere-asthenosphere boundary (Fig. 3). Grain size variations in the asthenospshere are relatively small and depend somewhat on the assumed parameters, especially the pressure dependent viscosity. The shallow part is not well constrained because of the complex mechanical behavior at low temperatures and high stresses. Thus, the most reliable estimates are, perhaps from about 50 km to 200 km. Those depend largely on the magnitude of lithospheric thickness variations.
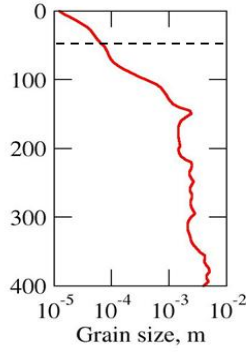
Fig. 3: Grain size variations in the convective subli-thospheric region. The dashed line indicates an approx-imate limit of applicability of grain size calculations. The grain size gradient depends largely on stress varia-tions which in turn depend largely on the amplitude of lithospheric thickness variations. The temperature ef-fect (de Bresser et al 1998; Shimizu, 1998, 2008, 2011; Austin and Evans 2007) is relatively small and cer-tainly not dominant as in models which assumed con-stant stress (Podolefsky et al 2004, Behn et al 2009).
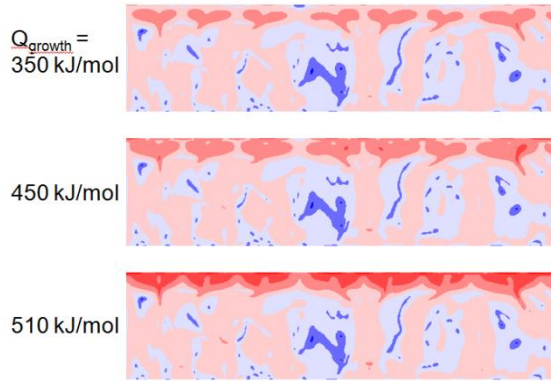

Fig.4: Two-dimensional grain size variations below the oceanic lithosphere for three different values of activa-tion energy for grain growth (activation energy for creep is 510 kJ/mol). The spacing of color bands is logarithmic and corresponds to one order of magnitude variation in grain size.

Seismic velocities

Grain size variations affect seismic velocities and at-tenuation (Karato 1993; Faul and Jackson 2005; Jack-son and Faul 2010), and thus the large grain size gra-dients generate correspondingly large seismic velocity gradients at the base of the lithosphere (Figs. 5,6). The decrease of the grain size in the direction from the mantle into the slab effectively serves as a melt barrier and may facilitate formation of a partially molten re-gion below the lithosphere. This may at least partially

contribute to the origin of the observed sharp lithos-phere-asthenosphere boundary (Kawakatsu et al. 2009).
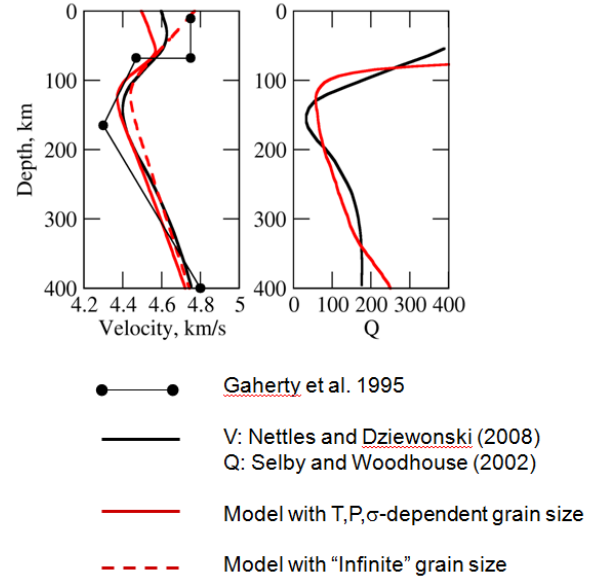

Fig.5: Seismic velocity and attenuation below the oceanic lithosphere. The relationships between seismic velocities, attenuation and grain size are from (Jackson and Faul 2010). These relationships give a significant-ly lower sensitivity of seismic velocities to grain size than the earlier model (Faul and Jackson 2005) be-cause of the elimination of non-physical grain-size dependence of unrelaxed (that is "normal" or at infinite frequencies) shear modulus which was originally present in (Faul and Jackson 2005).
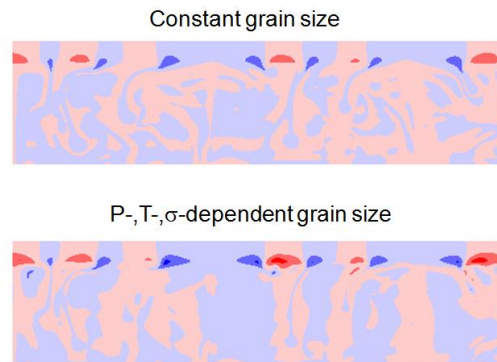

Fig.6: Comparison between seismic velocity anomalies without grain size variations and with self-consistent grain size variations (color change corresponds to 1% velocity difference; blue corresponds to large grain size, red - small grain size).

To see how the seismic image of a subducting slab is affected by grain size variations, we apply the same procedure to the subducting slab (Figs. 7, 8). Although there is some effect, it is probably small.
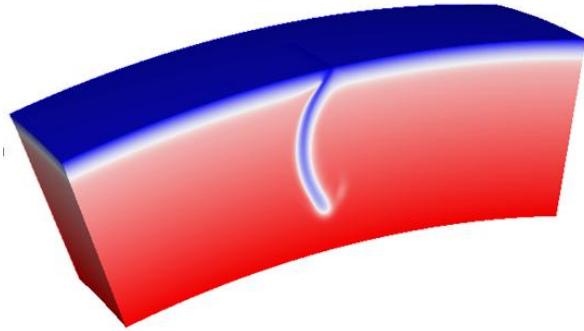

Fig.7: Temperature field in a three-dimensional model of subduction (courtesy of M. Morishige).
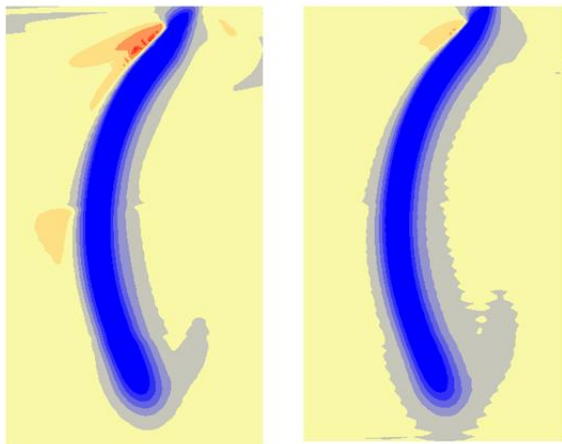

Fig.8: Seismic velocity anomalies for constant grain size (left) and self-consistently calculated grain size (right) in the subducting slab.

Conclusions

The grain size variations in the lower part of the lithosphere is largely controlled by stresses associated with varying lithospheric thickness. These variations are due to thernal thinning of the lithosphere by sublithospheric small-scale convection (including plumes). The recently proposed temperature dependence has a relatively small effect on the grain size. Grain size can be "seen" in seismic attenuation in low Q regions such as asthenosphere. The effect on seismic velcties in the asthenosphere and subducting slabs is relatively mild and would probably be hard to distinguish from other effects such as water and melting.

References

Austin, N. J., Evans, B., 2007, Paleowattmeters: a scaling relation for dynamically recrystallized grain size, Geology, 35, 343-346.

Behn, M. D., Hirth, G., and Elsenbeck J. R. II, 2009, Implications of grain size evolution on the seismic structure of the oceanic upper mantle, Earth Planet. Sci. Lett., 282, 178-189.

Bercovici, D., and Ricard, Y, 2005, Tectonic plate generation and two-phase damage: Void growth versus grain size reduction, J. Geophys. Res., 110, doi:10.1029/2004JB003181.

de Bresser, J. H. P., Peach, C. J., Reijs, J. P. J., and Spiers, C. J., 1998, On dynamic recrystallization during solid state flow: effects of stress and temperature, Geophys. Res. Lett., 25, 3457-3460.

Gaherty, J. B., T. H. Jordan, and L. S. Gee, 1996, Seismic structure of the upper mantle in a central Pacific corridor, J. Geophys. Res., 101, 22291– 22309.

Hall, C. E., and Parmentier, E. M. 2003, Influence of grain size evolution on convective instability. Geochem. Geophys. Geosyst., 4, doi:10.1029/2002GC000308.

Honda, S., 2009, Numerical simulations of mantle flow around slab edges, Earth Planet. Sci. Lett., 277, 112-122.

Jackson, I., and Faul, U. H., 2010, Grain size-sensitive viscoelastic relaxation in olivine: Towards a robust laboratory-based model for seismological application, Phys. Earth Planet. Inter., 183, 151-163.

Karato, S.-I., 1984, Grain-size distribution and rheology of the upper mantle, Tectonophys., 104, 155-176.

Karato, S., 1993, Importance of anelasticity in the interpretation of seismic tomography, Geophys. Res. Lett., 20, 1623-1626.

Karato, S., 2008, Deformation of Earth Materials, New York, Cambridge Univ., 463 pp.

Kawakatsu, H. et al., 2009, Seismic evidence for sharp lithosphere-asthenosphere boundaries of oceanic plates, Science, 324, 499-502.

Korenaga, J., 2005, Firm mantle plumes and the nature of the core-mantle boundary region, Earth Planet. Sci. Lett., 232, 29-37.

Long, M. D., and Silver, P., 2008, The subduction zone flow field from seismic anisotropy: A global view, Science, 319, 315-318.

Minster, B., and Anderson, D., 1981, A model of dislocation-controlled rheology for the mantle, Phil. Trans. R. Soc. Lond., 299, 319–356.

Nettles, M., and A. M. Dziewonski, 2008, Radially anisotropic shear-velocity structure of the upper mantle globally and beneath North America, J. Geophys. Res, 113, doi:10.1029/2006JB004819.

Podolefsky, N. S., Zhong, S., McNamara, A. K., 2004, The anisotropic and rheological structure of the oceanic upper mantle from a simple model of plate shear. Geophys. J. Int., 158, 287-296.

Riedel, M. R., and S. Karato, 1997, Grain-size evolution in subducted oceanic lithosphere associated with the olivine-spinel transformation and its effects on rheology, Earth Planet. Sci. Lett., 148, 27-43.

Selby N.D, and J. H. Woodhouse, 2002, The Q structure of the upper mantle: constraints from Rayleigh wave amplitudes, J. Geophys. Res. 107, doi:10.1029/2001JB000257.

Shimizu, I., 1998, Stress and temperature dependence of recrystallized grain size: A subgrain misorientation model, Geophys. Res. Lett., 25, 4237-4240.

Shimizu, I., 2008, Theories and applicability of grain size piezometers: The role of dynamic recrystallization mechanisms, J. Struct. Geol., 30, 899-917.

Shimizu, I., 2011, Steady-state grain size in dynamic recrystallization of minerals, in Recrystallization, in press.

Solomatov, V., 2001, Grain size-dependent viscosity convection and the thermal evolution of the Earth, Earth Planet. Sci. Lett., 191, 203-212.

Solomatov, V. S. and Moresi, L.-N., 2000, Scaling of time-dependent stagnant lid convection: Application to small-scale convection on the Earth and other terrestrial planets, J. Geophys. Res., 105, 21,795-21,818.

Solomatov, V. S., and Reese, C. C., 2008, Grain size variations in the Earth's mantle and the evolution of primordial chemical heterogeneities, J. Geophys. Res., 113, doi:10.1029/2007JB005319.

Wada, I., Behn, M. D., and He, J., 2011, Grain size distribution in the mantle wedge subduction zone, J. Geophys. Res., 116, doi:10.1029/2011JB008294.

2. Localized subcritical convective cells in temperature-dependent viscosity fluids

Introduction

Although most studies of thermal convection on Earth focus on well-developed, often very high Rayleigh number convection, low Rayleigh number convection is important for the understanding of the dynamics of small planetary objects, especially Mercury (Redmond and King 2007; King 2008) and icy satellites (McKinnon 1999; Barr and Pappalardo 2005; Barr and McKinnon 2007; Mitri and Showman 2008).

Low Rayleigh number convection in temperature-dependent viscosity fluids is complicated by the existence of subcritical solutions, that is at Rayleigh numbers below the critical Rayleigh number (Stengel et al. 1982; Richter et al. 1983; White 1988; Bottaro et al. 1992; Capone and Gentile 1994; Solomatov and Barr 2006, 2007). Although convection below the critical Rayleigh number may sound confusing, it might be worth emphasizing that, by definition, this number predicts the onset of convection for infinitesimal perturbations. When the amplitude of the perturbations is large finite-amplitude perturbations, steady-state or other types of non-decaying motions can exist even below the critical Rayleigh number (subcritical convection). This was shown theoretically (Segel and Stuart 1962; Segel 1965; Busse, 1967), observed in laboratory experiments (Stengel et al. 1982; Richter et al. 1983; White 1988) and studied numerically (Solomatov and Barr 2006; 2007). A schematic illustration of the bifurcation diagram for temperature-dependent viscosity convection is shown in Fig. 1.

Subcritical convection is poorly understood. Solomatov and Barr (2006, 2007) gave estimates of the absolute minimum critical Rayleigh number below which all convective motions decay and put some constraints on how the onset of convection depends on the initial finite-amplitude perturbations. Here we report a new type of convective planform for temperature-dependent viscosity convection - a spatially localized non-decaying convective cell which is only stable in the subcritical region. Previous studies showed that in the vicinity of the critical Rayleigh number, the convective planform occupies the entire fluid layer and it usually takes a form of hexagons, squares or rolls or a mixture of these patterns (Chandrasekhar 1961; Busse 1967; Richter et al. 1983; White 1988). Localized structures were observed in other systems far from equilibrium (Thual and Fauve 1988; van Saarloos and Hohenberg 1992). What follows below is probably the first report of spatially localized convective cells for purely ther-

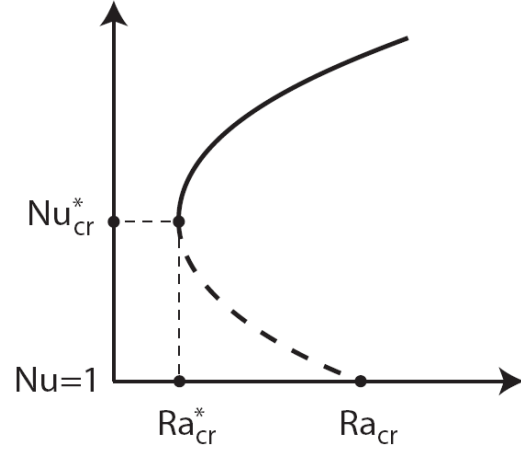mal convection, with localization being caused by temperature-dependent viscosity.

Fig. 1: Schematic illustration of the bifurcation diagram for temperature-dependent viscosity convection in Ra-Nu axes. The point $Ra=Ra_{cr}$, $Nu=1$ is a subcritical pitchfork bifurcation. The point $Ra=Ra^*_{cr}$, $Nu=Nu^*_{cr}$ is a saddle-node bifurcation. The Rayleigh number Ra_{cr} is the usual critical Rayleigh number predicted by the linear theory. The Rayleigh number Ra^*_{cr} is the absolute minimum critical Rayleigh number. At $Ra > Ra_{cr}$, the conductive solutions, $Nu=1$, are unstable to infinitesimal perturbations. Between $Ra=Ra^*_{cr}$ and $Ra=Ra_{cr}$ the conductive solutions are stable to infinitesimal perturbations but unstable to finite amplitude perturbations. Stable steady-state finite-amplitude convection solutions are located on the solid line with stable subcritical solutions are located between Ra^*_{cr} and Ra_{cr}. Unstable steady-state finite-amplitude solutions are located on the heavy dashed line (the unstable subcritical branch) which connects the two bifurcation points. At $Ra < Ra^*_{cr}$ all convective motions eventually decay.

Model

Two-dimensional calculations are performed in a box of depth d and length l. Three-dimensional calculations are performed in a box of depth d and equal width and length l. In all cases, the upper and lower boundaries are maintained at constant temperatures and the vertical boundaries are thermally insulated. The boundaries are either free-slip or no-slip, as described below. The non-dimensional temperatures of the upper and lower boundaries are 0 and 1 respectively. The non-dimensional equations of thermal convection in the Boussinesq approximation and for infinite

Prandtl number are solved with Citcom (Moresi and Solomatov 1995).

The viscosity function is either exponential or super-exponential. Exponential function is a Frank-Kamenetskii approximation to the Arrhenius viscosity of rocks, which is valid in the limit of very large viscosity contrasts (Morris 1982; Morris and Canright 1984; Ansari and Morris 1985; Fowler 1985; Reese et al. 1999). The viscosity contrast between the boundaries is 10 orders of magnitude. This is at least 4 orders of magnitude higher than the transition to the stagnant lid regime (Solomatov 1995; Moresi and Solomatov 1995) and thus it ensures a well-developed stagnant lid regime. This also creates a significant interval of Rayleigh numbers where the subcritical convection exist. The super-exponential function represents the viscosity of golden syrup (Richter et al. 1983). This viscosity law is chosen so that the numerical results can be tested in future laboratory experiments. The exponential viscosity models are calculated with free-slip boundary conditions while the super-exponential viscosity models are calculated with no-slip boundary conditions. In both cases, the vertical boundaries are free-slip.

Results

Subcritical localized cell solutions for exponential viscosity in 2D and 3D are shown in Figures 2 and 3, respectively. The region of stability of 3D localized cells is shown in Nu-Ra axes in Fig. 4. Subcritical localized cell solutions for super-exponential viscosity in 2D and 3D are shown in Figs. 5 and 6, respectively. The region of stability of 3D localized cells is shown in Fig. 7. An interesting difference from the exponential viscosity case (free-slip boundaries) is that in the super-exponential case (no-slip boundaries) an array of very weak secondary convective cells (rolls in 2D and tori in 3D) form next to the main cell. Also, 3D localized cell solutions appear to be stable at Rayleigh numbers which are slightly lower than those obtained in 2D calculations.
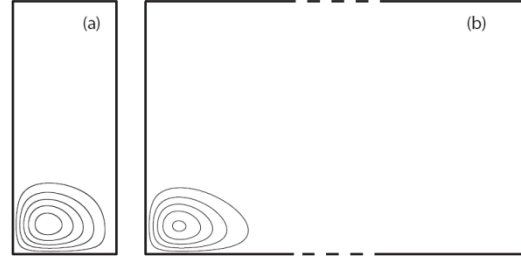

Fig. 2: Streamlines for stable steady-state two-dimensional solutions near the absolute minimum critical Rayleigh number. (a) Aspect ratio a=0.41. (b) Aspect ratio a>1.5. The solutions are indistinguishable from a=1.5 to the maximum tested aspect ratio a=6.
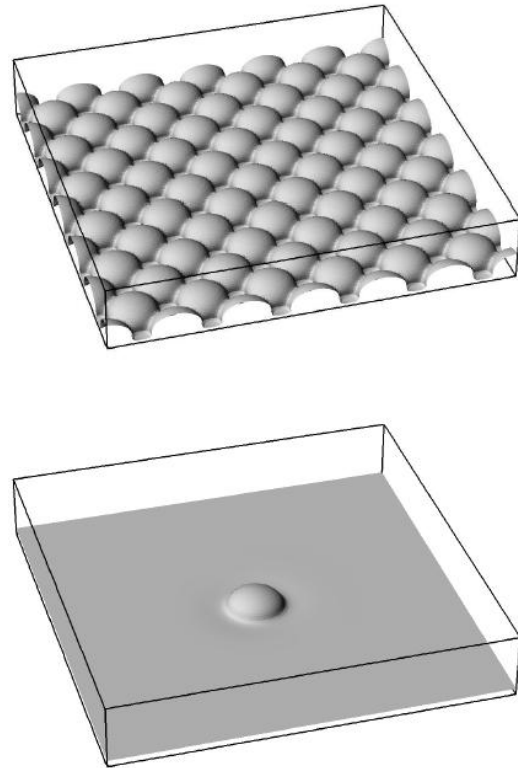

Fig. 3: Top: An isosurface T=0.9 showing a subcritical convection planform consisting of a stable square array of convective cells in a 6x6x1 box with free-slip boundaries and exponential viscosity. Bottom: A steady-state localized convective cell at the same Rayleigh number. Other subcritical localized solutions are very similar in their appearance.
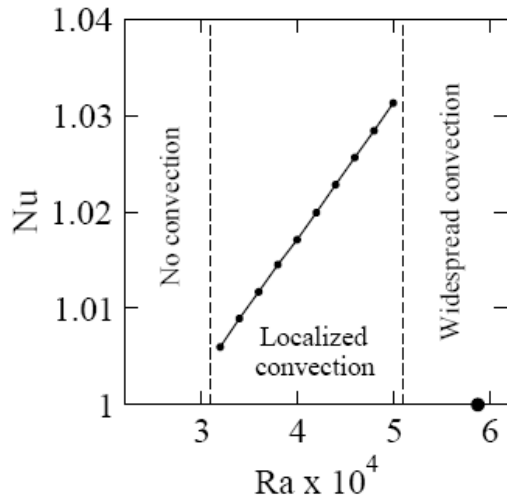
Fig. 4: Nusselt number as a function of Rayleigh number for localized cell solutions in a 6x6x1 box with exponential viscosity. The solid circle shows the location of the critical Rayleigh number. The boundaries of the stability of localized solutions are approximately shown with vertical dashed lines.
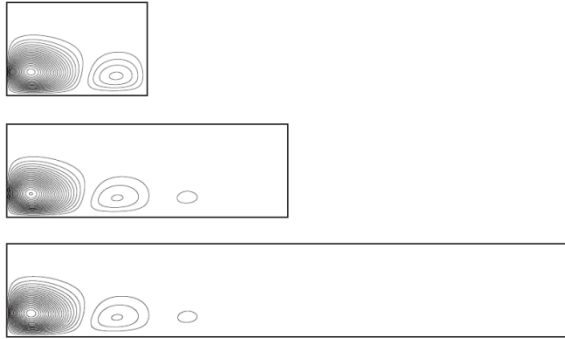

Fig. 5: Streamlines for stable steady-state solutions near the critical point for golden syrup (super-exponential) viscosity and no-slip boundaries. The aspect ratios are (from top to bottom) a=1.5, 3 and 6.
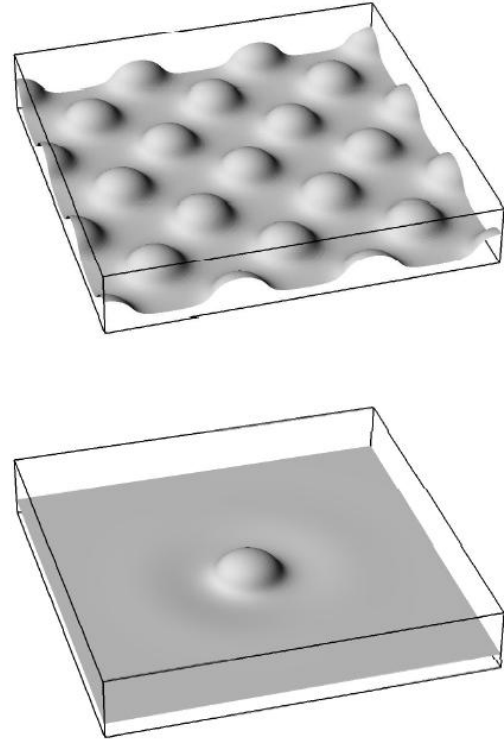

Fig. 6: Top: An isosurface T=0.75 showing a subcritical convection planform consisting of a stable square array of convective cells in a 6x6x1 box for super-exponential viscosity (golden syrup) and no-slip boundaries. Bottom: A steady-state localized convective cell at the same Rayleigh number. Other subcritical localized solutions are very similar in their appearance.
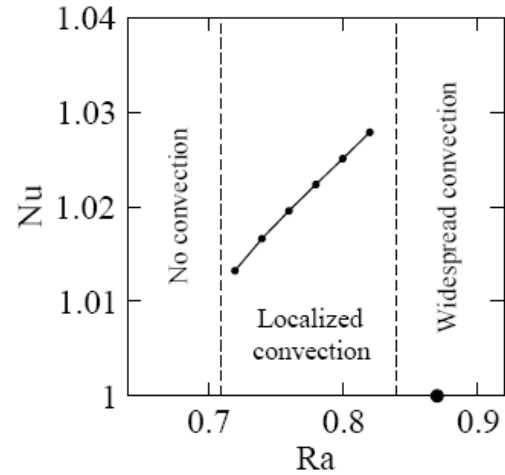

Fig. 7: Nusselt number as a function of Rayleigh number for localized cell solutions in a 6x6x1 box with super-exponential viscosity. The solid circle shows the location of the critical Rayleigh number. The bounda-

ries of the stability of localized solutions are approximately shown with vertical dashed lines.

Conclusions

Numerical simulations of temperature-dependent viscosity convection reveal a new type of convective planform - a single, spatially localized convective cell. The cell has a shape of a symmetric circular dome with an upwelling at the center. This solution is stable at subcritical Rayleigh numbers, that is below the critical Rayleigh number for linear onset of convection. This type of convective solutions is in stark contrast with the usual, supercritical convection, where the convective cells form through the entire layer and the spacing between the cells is of the order of the layer thickness. The existence of stable localized subcritical cells raises some interesting questions. If this type of solutions exists for relatively simple, temperature-dependent viscosity, it must exist for more complex viscosities such as grain-size dependent viscosity, power-law viscosity and plastic yielding. Power-law viscosity convection is particularly intriguing because it is subcritical at all Rayleigh numbers and therefore it must have a significantly larger span of the subcritical region where localized convection cells are stable. The interaction between the cells is another interesting question. Even though the interaction is extremely weak, the dynamics of cell interaction and pattern formation might be very complex as it is the case for other systems far from equilibrium (Cross and Hohenberg 1993). Numerical investigation of these problems will be computationally challenging because of the slow dynamics and the need for a high resolution because of the extreme viscosity variations. For example, the simulations presented here had to be run tens and hundreds of diffusion times. This is several orders of magnitude longer than typical simulations of thermal convection (a fraction of diffusion time). One of the implications of the existence of subcritical localized convective cells for planetary geodynamics is that a convective upwelling can be a localized phenomenon without any special conditions such as lateral heterogeneity or laterally varying heating. Also, the spacing between the isolated cells can be arbitrarily large. It is controlled not by the thickness of the convective layer but by the initial conditions. This type of convection may be responsible for various spatially localized tectonic features such as coronas on Venus and chaos regions on Europa.

References

Ansari A., Morris, S., 1985. The effects of a strongly temperature-dependent viscosity of Stokes drag law: Experiments and theory. J. Fluid Mech. 10, 459-476.

Barr, A. C., Pappalardo, R. T., 2005. Onset of convection in the icy Galilean satellites: Influence of rheology, J. Geophys. Res. 110, 10.1029/2004JE002371.

Barr, A. C., McKinnon, W. B. 2007. Convection in Enceladus' ice shell: Conditions for initiation. Geophys. Res. Lett. 34, 10.1029/2006GL028799.

Behounkova, M, Choblet, G., 2009. Onset of convection in a basally heated spherical shell, application to planets. Phys. Earth Planet. Inter. 176, 157-173.

Bottaro, A., Metzener, P., Matalon, M., 1992. Onset and two-dimensional patterns of convection with strongly temperature-dependent viscosity. Phys. Fluids 4, 655-663.

Busse, F.H., 1967. The stability of finite amplitude cellular convection and its relation to an extremum principle. J. Fluid Mech. 30, 625-649.

Capone, F., Gentile, M. 1994. Nonlinear stability analysis of convection for fluids with exponentially temperature-dependent viscosity. Acta Mech. 107, 53-64.

Chandrasekhar, S., Hydrodynamic and Hydromagnetic stability. Oxford, pp. 654, 1961.

Fowler, A.C., 1985. Fast thermoviscous convection. Stud. Appl. Math. 72, 189-219.

Cross, M.C., Hohenberg, P.C., 1993. Pattern formation outside of equilibrium. Rev. Mod. Phys. 65, 851-1112.

King, S. D., 2008, Pattern of lobate scarps on Mercury's surface reproduced by a model of mantle convection. Nature Geoscience 1, 229-232.

McKinnon, W.B., 1999. Convective instability in Europa's floating ice shell. Geophys. Res. Lett. 26, 951-954.

Mitri, G., Showman, A.P., 2009. Thermal convection in ice-I shells of Titan and Enceladus. Icarus, 193, 387-396.

Morris, S., 1982. The effects of strongly temperature-dependent viscosity on slow flow past a hot sphere. J. Fluid Mech. 124, 1-26.

Richter, F.M., Nataf, H.C., Daly, S., 1983. Heat transfer and horizontally averaged temperature of convection with large viscosity variations. J. Fluid. Mech. 129, 173-192.

Segel, L.A., 1965. The non-linear interaction of of a finite number of disturbances to a layer of fluid heated from below. J. Fluid Mech. 21, 359-384.

Segel, L.A., Stuart, J.T., 1962. On the question of the preferred mode in cellular thermal convection. J. Fluid Mech. 13, 289-306.

Solomatov, V.S., Scaling of temperature- and stress-dependent viscosity convection. Phys. Fluids 7, 266-274, 1995.

Solomatov, V. S., Barr, A. C. 2006. Onset of convection in fluids with strongly temperature-dependent, power-law viscosity. Phys. Earth Planet. Inter. 155, 140-145.

Solomatov, V. S., Barr, A. C. 2008. Onset of convection in fluids with strongly temperature-dependent, power-law viscosity: 2. Dependence on the initial perturbation. Phys. Earth Planet. Inter. 165, 1-13.

Solomatov, V.S., Zharkov, V. N., 1990. The thermal regime of Venus. Icarus 84, 280-295.

Stengel, K.C., Oliver, D.C., Booker, J.R., 1982. Onset of convection in a variable viscosity fluid. J. Fluid. Mech. 120, 411-431.

Thual, O., Fauve, S., 1988. Localized structures generated by subcritical instabilities. J. Phys. France 49, 1829-1833.

van Saarloos, W., Hohenberg, P.C., 1992. Fronts, pulses, sources and sinks in generalized complex Ginzburg-Landau equations. Physica D 56, 303-367.

White, D.B. 1988. The planforms and onset of convection with a temperature-dependent viscosity. J. Fluid. Mech. 191, 247-286.